Soil hydraulic properties determined by inverse modeling of drip infiltrometer experiments extended with pedotransfer functions

Kotlar, Ali Mehmandoost; Varvaris, Ioannis; de Jong van Lier, Quirijn; de Jonge, Lis Wollesen; Møldrup, Per; Iversen, Bo V.

Published in:
Vadose Zone Journal

DOI (link to publication from Publisher):
10.2136/vzj2018.12.0215

Publication date:
2019

Document Version
Publisher's PDF, also known as Version of record

Published July 18, 2019

Original Research

Core Ideas

- A robust PTF was developed to predict water contents at −1, −10, and −158 m tension.
- Drip infiltrometer experiments were inversely modeled to predict soil hydraulic properties.
- Both θ(*h*) and *K*(*h*) can be accurately estimated from experimental data together with PTFs.

Soil Hydraulic Properties Determined by Inverse Modeling of Drip Infiltrometer Experiments Extended with Pedotransfer Functions

Ali Mehmandoost Kotlar,* Ioannis Varvaris, Quirijn de Jong van Lier, Lis Wollesen de Jonge, Per Møldrup, and Bo V. Iversen

A transient flow experiment using automated drip infiltrometers (ADIs) was performed on soil columns (about 6 dm^3) large enough to incorporate macropore flow effects. We investigated to what extent the estimated soil hydraulic parameters obtained from inverse modeling of these experiments are reliable. A machine learning based pedotransfer function (PTF) for prediction of water content at −1, −10, and −158 m pressure head was developed. Sensitivity analysis of the van Genuchten parameters (residual and saturated water content θ_r and θ_s, fitting parameters α, n, and λ, and saturated hydraulic conductivity K_s) in soils of sandy, silty, and clayey textures showed that the temporal variation of pressure heads in ADI scenarios was not sensitive to θ_r and θ_s. The other parameters were accurately estimated from numerically synthesized data. The uniqueness of the estimated parameters did not change when a bias, representing experimental error, was added to the data set. In actual columns, using the temporal and spatial pressure head data from the ADIs and the water contents in the drier range predicted by the developed PTF resulted in a precise estimation of the van Genuchten parameters. Not including the PTF water contents resulted in nonuniquely estimated van Genuchten parameters.

Abbreviations: ADI, automated drip infiltrometer; GPR, Gaussian process regression; MSPE, mean square percentage error; NSE, Nash–Sutcliffe efficiency; PTF, pedotransfer function; RMSE, root mean square error; SHP, soil hydraulic property; VG, van Genuchten.

A.M. Kotlar and Q. de Jong van Lier, Univ. of São Paulo, Centre for Nuclear Energy in Agriculture (CENA/USP), Caixa Postal 96, 13416-903, Piracicaba (SP), Brazil; A.M. Kotlar, I. Varvaris, L.W. de Jonge, and B.V. Iversen, Dep. of Agroecology, Aarhus Univ., Blichers Allé 20, 8830 Tjele, Denmark; P. Møldrup, Dep. of Civil Engineering, Aalborg Univ., Thomas Manns Vej 23, 9220 Aalborg, Denmark. *Corresponding author (aliko@usp.br).

Received 20 Dec. 2018.
Accepted 25 May 2019.

Citation: Kotlar, A.M., I. Varvaris, Q. de Jong van Lier, L.W. de Jonge, P. Møldrup, and B.V. Iversen. 2019. Soil hydraulic properties determined by inverse modeling of drip infiltrometer experiments extended with pedotransfer functions. Vadose Zone J. 18:180215. doi:10.2136/vzj2018.12.0215

The accurate modeling of water flow and budgeting of solute and heat transport in the vadose zone based on a numerical solution of the Richards equation depends on precise knowledge of the fundamental soil hydraulic properties (SHPs): water retention [θ(*h*)] and hydraulic conductivity [*K*(*h*)] (Groh et al., 2018; Weninger et al., 2018). Direct measurement of *K*(*h*) is laborious, therefore *K*(*h*) is most commonly indirectly derived by using the measured saturated hydraulic conductivity, the θ(*h*) function, and an empirical parameter related to tortuosity and connectivity, which, in its turn, exhibits a very large spatial variability (Durner et al., 1999). Consequently, any method to directly quantify *K*(*h*) represents an improvement of modeling quality, but this is predominantly neglected (Weninger et al., 2018; Weller et al., 2011).

Both soil heterogeneity at different scales, from millimeters to kilometers, and the large amount of required data restrict the use of pedotransfer functions for the determination of SHPs and especially the soil water retention function [θ(*h*)] (Graham et al., 2018). Methods to measure SHPs, including pressure plates and in situ techniques like internal drainage experiments, are commonly laborious and costly. Most of these methods are inadequate to describe water dynamics at larger scales because they require hydraulic equilibrium, restricting experiments to small sample sizes (Scharnagl et al., 2011). A proper and real estimation of SHPs requires experiments performed on sample sizes larger than the representative elementary volume under transient water flow conditions. Subsequent inverse modeling of the observed data allows hydraulic properties to be effectively lumped

for the scale of interest (Hopmans et al., 2002; Mallants et al., 1997; Pachepsky and Hill, 2017).

Numerical methods to inversely model transient flow methods under diverse boundary conditions have recently gained considerable attention (Li et al., 2018; Rashid et al., 2015; Arora et al., 2011). In the upward infiltration method, a constant upward flux from the bottom is established as a boundary condition to obtain SHPs in the wetting branch. This method was proposed by Hudson et al. (1996) and modified through an applied constant bottom suction, allowing the cumulative flux data to be included as an auxiliary variable in the objective function (Young et al., 2002). The latest improvement in the upward infiltration method was to impose multiple tensions at the lower boundary (Moret-Fernández et al., 2016) and estimate SHPs without using tensiometers but small ring soil cores (100 cm^3).

Another boundary condition is established in evaporation scenarios, initially proposed on horizontal (Gardner and Miklich, 1962) and vertical columns (Wind, 1969) and now frequently used for the simultaneous determination of retention and conductivity functions (Šimůnek et al., 1998; Romano and Santini, 1999; Schelle et al., 2011). These methods tend to fail in providing conductivities under near-saturated conditions.

Outflow experiments inversely model the measured outflow of water from a soil sample under established pressure or suction conditions. For instance, inverse modeling of one-step outflow experiments (Kool et al., 1985) supplied with further information of water content (van Dam et al., 1992) was improved by multistep outflow experiments (van Dam et al., 1994).

Similar to outflow experiments, a group of methods is based on the crust method (Bouma and Baker, 1974), in which vertical flow is established under a gravitational gradient alone, without a pressure head gradient. As an alternative to the original crust method, which requires a semi-infinite soil column, automated drip infiltrometers (Iversen et al., 2004) allow similar boundary conditions in a finite geometry. In automatic drip infiltrometer (ADI) experiments, data on K(h) can be obtained for the wet range. The extension of these pressure head data with information on water content may improve the well-posedness of the inverse modeling problem (Zhang et al., 2003). The objective of this study was to analyze ADI experimental data using inverse modeling techniques and to investigate if the extension of retention data to the drier range using prediction by a Gaussian process regression pedotransfer function trained on a local data set may result in a better assessment of SHPs.

Materials and Methods

Sampling and Experimental Setup

Fifteen undisturbed soil columns (20 cm high and 20 cm in diameter, volume 6.283 dm^3) were sampled from the top layer of an experimental field located in Lund, Denmark (coordinates 55.24 N, 12.29 E), which belongs to the Danish Pesticide Leaching Assessment Program (Lindhardt et al., 2001). The soil has a sandy loam texture (64% sand, 23% silt, and 13% clay, 2.5% organic matter content) (Kotlar et al., 2019a). Winter wheat was cultivated at the location during the 5 yr before sampling. In the same field, small ring samples (100 cm^3) were taken for water retention analysis using a sand box for pressure heads from −0.1 to −1 m and ceramic plate equipment for pressure heads between −1.6 and −150 m. Water content for the very dry soil was determined after one night of oven drying using a WP4-T dewpoint potentiometer (METER Group).

Analogous to the studies of McKenzie et al. (2001) and Weller et al. (2011), unsaturated hydraulic conductivity was measured using automated (step flow) drip infiltrometers (Fig. 1) as reported by Iversen et al. (2004). In the ADI setup, tensiometers recorded pressure heads at five depths in the column under step flow. A suction was applied at the bottom of the sample, and the inflow was adjusted until a steady state was established in which the five tensiometers showed similar readings and flow was due to a gravitational gradient only. Subsequently, suction was increased and the process repeated. Five to eight bottom suctions were applied, varying between −0.1 to −1 m pressure head, allowing determination of $K(h)$ in this range of pressure heads. Saturated hydraulic conductivity was independently measured using the constant-head method as described by Iversen et al. (2004).

Generation of Synthetic Data

To evaluate the reliability of the SHPs estimated by inverse modeling of ADI scenarios, ADI experiments similar to the

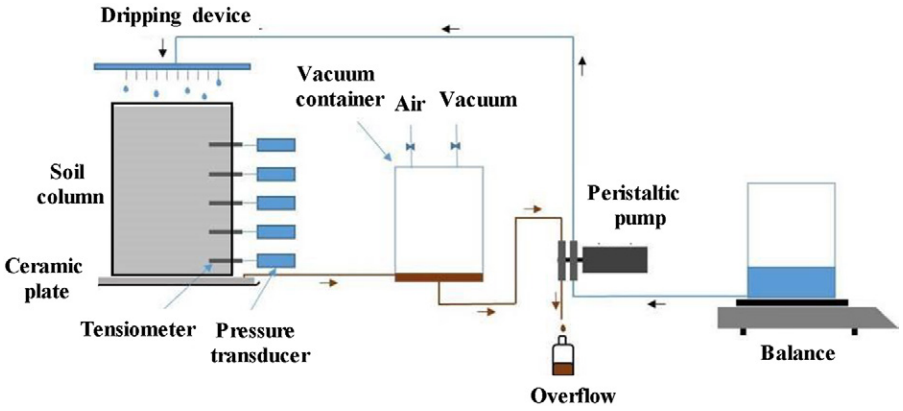

Fig. 1. Schematic design of the automatic drip infiltrometer (ADI) apparatus for measuring unsaturated hydraulic conductivity.

experimental setup were simulated numerically by HYDRUS-1D for three reference soils used by Vrugt et al. (2001) (Table 1).

The HYDRUS-1D model numerically simulates the temporal and spatial changes in water content or pressure head by solving the Richards equation (Šimůnek et al., 2008):

$$\frac{\partial \theta}{\partial t} = \frac{\partial}{\partial z}\left[K(h)\frac{\partial h}{\partial z} + K(h) \right] \quad [1]$$

where θ is the volumetric soil water content, t is time (s), z is the vertical space coordinate (cm), K is the hydraulic conductivity (cm s^{-1}), and h is pressure head (cm). The soil hydraulic properties were modeled using the van Genuchten–Mualem constitutive relationships (van Genuchten, 1980):

$$S_e(h) = \frac{\theta(h) - \theta_r}{\theta_s - \theta_r} = \left(1 + |\alpha h|^n\right)^{-m} \quad [2]$$

$$K(h) = K_s S_e^{\lambda}\left[1 - \left(1 - S_e^{1/m}\right)^m\right]^2 \quad [3]$$

where S_e is the saturation degree, θ_s and θ_r are volumetric saturated and residual water contents, and α (cm^{-1}), $m = 1 - 1/n$, and λ are fitting parameters.

The simulated scenarios were chosen to represent the ADI experiment in 20-cm-high soil columns with three tensiometers (at depths of 7, 10, and 13 cm), discretized into 100 elements. A finer grid size was chosen near the virtual tensiometers. At the bottom of the soil column, a 1-cm-thick porous plate with K_s equal to 2.7 cm d^{-1} was simulated with van Genuchten (1980) parameters n = 1.001 and α = 10^{-20} cm^{-1}, thus ensuring that it remained fully saturated for the pressure heads applied (Šimůnek et al., 2008). Boundary conditions were multistep flux [always less than K(−1 cm)] and zero evaporation. The bottom boundary condition was a stepwise varying pressure head, never lower than −100 cm.

Sensitivity Analysis

To study the parameter sensitivity of the described ADI scenario and to evaluate if insensitive parameters might be removed (Ritter et al., 2003; Lambot et al., 2004), one-parameter analyses as well as two-parameter analyses were performed using the same scenarios described for synthetic data generation. In the one-parameter analysis, 100 forward simulations (Monte Carlo) were performed by changing one of the parameters θ_r, θ_s, α, n, λ, or K_s within an interval around the respective true value. Similarly, in the two-parameter analysis, parameter pairs α–n, α–K_s, α–λ, n–K_s and n–λ were simultaneously changed, resulting in 100 × 100 = 10,000 realizations. The two-parameter analyses allowed assessment of the corresponding response surfaces. In both one- and two-parameter analyses, the remaining parameters were kept at their true value.

Two statistical indicators were used to compare the Monte Carlo realizations of simulated pressure head readings (h_{sim}) with the pressure heads simulated with the reference values (h_{ref}): the root mean square error (RMSE) and the Nash–Sutcliffe efficiency (NSE), where s is the number of samples:

$$\mathrm{RMSE} = \sqrt{\frac{\sum_{i=1}^{s}(h_{sim} - h_{ref})^2}{s-1}} \quad [4]$$

$$\mathrm{NSE} = 1 - \frac{\sum_{i=1}^{s}(h_{sim} - h_{ref})^2}{\sum_{i=1}^{s}(h_{ref} - \bar{h}_{ref})^2} \quad [5]$$

Inverse Modeling

The inverse modeling to obtain the SHP functions θ(h) and K(h) aimed to minimize the following objective function F(∅):

$$\mathrm{F}(\varnothing) = \sum_{j=1}^{p}\sum_{i=1}^{s}\left\{\left[\varnothing_k^{obs}(z_j, t_i) - \varnothing_k^{sim}(z_j, t_i)\right]^2\right\} \quad [6]$$

where $\varnothing_k^{obs}$ and $\varnothing_k^{sim}$ are the observed and simulated values, respectively, of a target parameter (e.g., pressure head) at depth z_j and time t_i. Minimization of the objective function was performed using HYDRUS-1D (Šimůnek et al., 2008). HYDRUS-1D uses the Levenberg–Marquardt non-linear minimization method, a local gradient-type search algorithm, as opposed to global search algorithms that search the entire parameter space. Local search algorithms are generally sensitive to the initial parameter estimates (Šimůnek et al., 2005; Kelleners et al., 2005).

To reduce the number of parameters to be estimated by inverse modeling, parameters θ_r and θ_s were fixed at experimentally observed values. Saturated water content was calculated based on bulk density and particle density (2650 kg m^{-3}). Estimated water content at pF = 5 using a WP4 psychrometric tensiometer was used as the residual water content. A stochastic bias was introduced, applying a 1-cm noise to the observed pressure heads to

Table 1. Soil hydraulic parameters for reference soils (extracted from Vrugt et al., 2001).

Soil texture	van Genuchten parameters†					
	θ_r	θ_s	α	n	K_s	λ
			cm^{-1}		cm d^{-1}	
Sand	0.02 (0–0.07)‡	0.38 (0.3–0.5)	0.0214 (0.001–0.03)	2.075 (1.4–3.0)	15.56 (7–50)	0.039 (−3–3)
Silt	0.034 (0–0.1)	0.46 (0.3–0.5)	0.0160 (0.001–0.04)	1.370 (1.2–1.9)	6.00 (4–25)	0.5 (−3–3)
Clay	0.00 (0–0.1)	0.42 (0.3–0.5)	0.0191 (0.009–0.09)	1.152 (1.1–2.5)	13.80 (7.5–35)	−1.384 (−3–3)

† θ_r, residual volumetric water content; θ_s, saturated volumetric water content; α, n, and λ, fitting parameters; K_s, saturated hydraulic conductivity.
‡ Values in parentheses represent the range of values used in one- and two-parameter Monte Carlo realizations.

evaluate the sensitivity to experimental errors (Kool and Parker, 1988; Peters and Durner, 2008).

In this study, two sets of data were used in inverse modeling to estimate the SHPs: (i) the traditional ADI data set consisting of measured pressure head data from the three most central tensiometers (eliminating the top and bottom tensiometers, thus avoiding possible boundary disturbance); and (ii) the ADI data set consisting of measured pressure head data from the three most central tensiometers extended with water contents predicted by a pedotransfer function.

The testing of inverse modeling and obtained parameters was accomplished by comparison of $K(h)$ observed in ADI experiments and simulated by estimated parameters using the RMSE and the mean square percentage error (MSPE):

$$\mathrm{MSPE} = \frac{100\%}{n}\sum_{i=1}^{s}\left(\frac{K_{\mathrm{sim},i} - K_{\mathrm{obs},i}}{K_{\mathrm{obs},i}}\right)^2 \quad [7]$$

where $K_{\mathrm{obs},i}$ is the ith hydraulic conductivity measured in the ADI experiment, $K_{\mathrm{sim},i}$ is the corresponding $K(h)$ calculated using parameters obtained by inverse modeling, and n is the number of observations. For the cases where water contents predicted by PTF and simulated ones obtained from the van Genuchten parameters or the measured ones from small rings were compared with each other, the RMSE was the evaluation criterion.

Pedotransfer Function for Water Contents

A machine learning based pedotransfer function (PTF) was developed by Gaussian process regression (GPR) to obtain retention data for the dry range. Gaussian process regression uses nearest neighbors, considering the distance between neighbors based on covariance (or kernel) function. Closeness or similarity between two points (distance) is given by kernel functions (Rasmussen and Williams, 2006). Kernel similarities between a test point and each point of the training data are found to predict the target of the test point, thus kernel values of far points approach zero. Briefly, the mathematical form of GPR is

$$\begin{bmatrix} Y_{\mathrm{tr}} \\ Y_{\mathrm{ts}} \end{bmatrix} = \mathrm{GP}\left(0, \begin{bmatrix} K_{\mathrm{tr}} & K_{\mathrm{trs}} \\ K_{\mathrm{trs}}^{\mathrm{T}} & K_{\mathrm{ts}} \end{bmatrix}\right) \quad [8]$$

where Y_{tr} and Y_{ts} are training and test targets (e.g., here water content points) and K_{tr} is the covariance of the training data, K_{ts} of the test data, and K_{trs} between test and training data. Considering a Gaussian likelihood function, the predictive mean y_{ts} for a given test point (x_{ts}) is

$$y_{\mathrm{ts}} = \mathbf{K}_{x_{\mathrm{ts}}}^{\mathrm{T}} K_{\mathrm{tr}}^{-1} Y_{\mathrm{tr}} \quad [9]$$

where $\mathbf{K}_{x\mathrm{ts}}{}^{\mathrm{T}}$ is the vector with the distances from x_{ts} to each training point. Optimization of kernel parameters and other details are explained in Kotlar et al. (2019a, 2019c).

The developed PTF allows prediction of water contents θ_{pF1}, θ_{pF2}, θ_{pF3} and $\theta_{\mathrm{pF4.2}}$ corresponding to pressure heads of −0.1 (pF1), −1 (pF2), −10 (pF3) and −158 m (pF4.2), respectively. For each water content (θ_{pF1}, θ_{pF2}, θ_{pF3} and $\theta_{\mathrm{pF4.2}}$), easily measurable soil properties including texture (sand, silt, and clay contents), organic matter, and bulk density (BD) were used as predictors. Gaussian process regression was trained by a random selection of 70% of the data set including 452 soils from Denmark retrieved from Kotlar et al. (2019b).

Considering the performance of the PTFs for the four tensions, some of them were selected to be used as additional data for the drier part in the inverse simulation.

Results and Discussion

Forward Modeling and Sensitivity Analysis

Table 2 shows averages of the statistical indicators RMSE and NSE of pressure heads for the 100 one-parameter Monte Carlo simulations performed for each van Genuchten (VG) parameter for the reference sand, silt, and clay soils from Table 1. Results show that the prediction of pressure head is relatively insensitive to the residual water content, corroborating the report by Kelleners et al. (2005), as well as to saturated water content. Higher sensitivity is shown for n, K_s, λ, and especially α.

For silt and clay soils, the model showed less sensitivity to λ compared with the sand soil. This could be expected because λ especially affects the prediction of $K(h)$ in the dry range, which occurs more commonly in ADI experiments in a sandy soil. Parameter α is the most sensitive parameter in the model for the sand and silt soils; this parameter strongly affects the pressure

Table 2. The RMSE and Nash–Sutcliffe efficiency (NSE) values of pressure heads obtained from simulations in sand, silt, and clay soil (Table 1) scenarios in 100 Monte Carlo realizations for each of the van Genuchten parameters. Average for pressure heads at three depths (7, 10, and 13 cm) compared with values obtained with the reference parameter set.

		van Genuchten parameters†					
Soil	Statistic	θ_r	θ_s	α	n	K_s	λ
Sand	RMSE, cm	1.2 (0.00)‡	1.5 (0.00)	25.2 (0.7)	3.5 (0.6)	9.2 (0.5)	9.9 (0.1)
	NSE	0.98 (0.00)	0.97 (0.01)	−5.38 (1.80)	0.82 (0.01)	0.09 (0.10)	−0.38 (0.28)
Silt	RMSE, cm	0.7 (0.00)	2.0 (0.0)	21.9 (2.0)	10.8 (1.0)	10.9 (0.6)	3.3 (0.3)
	NSE	0.99 (0.00)	0.95 (0.00)	−3.04 (1.23)	−0.04 (0.08)	−0.19 (0.00)	0.86 (0.03)
Clay	RMSE, cm	1.9 (0.9)	1.7 (1.1)	24.0 (12.5)	28.1 (3.2)	13.6 (6.5)	4.4 (2.8)
	NSE	0.98 (0.01)	0.98 (0.02)	−2.2 (1.90)	−3.6 (1.80)	0.0 (0.80)	0.88 (0.11)

† θ_r, residual volumetric water content; θ_s, saturated volumetric water content; α, n, and λ, fitting parameters; K_s, saturated hydraulic conductivity.
‡ Standard deviations in parentheses.

heads observed at the tensiometers. For the clay soil, the model is more sensitive to n. Sensitivity to λ was not significant for the clay soil (Table 2), but for the studied Danish soils, with sandy loam texture, λ was maintained as an optimization parameter.

The low sensitivity of θ_r and θ_s, added to the fact that they can be experimentally measured, made it advantageous to fix these parameters at their true values instead of inversely modeling them. Therefore, only the parameters α, n, λ, and K_s were optimized to obtain the soil water retention and hydraulic conductivity functions.

Results of the two-parameter sensitivity analyses are shown in Fig. 2. For n and α, any change in α leads to large variation in the objective

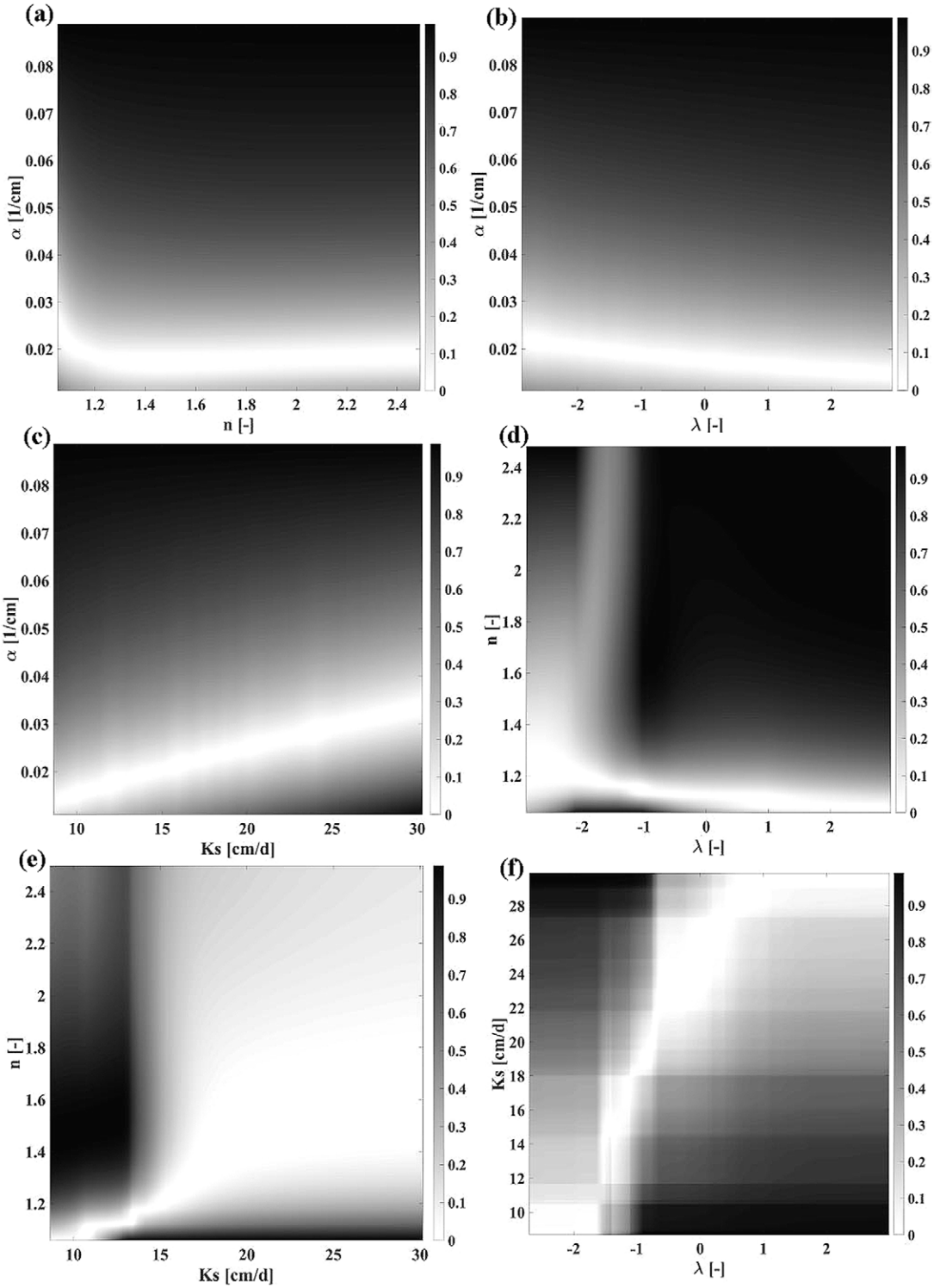

Fig. 2. Relative average RMSE (RMSE/RMSE$_{max}$) response surfaces (two-parameter sensitivity analysis) of the objective function for pressure heads at three depths for parameter pairs (a) α–n, (b) α–λ, (c) α–K_s, (d) n–λ, (e) n–K_s, and (f) K_s–λ, where α, n, and λ are fitting parameters and K_s is the saturated hydraulic conductivity.

function; however, n hardly affects the objective function and contours are parallel to the n axis (Fig. 2a). As a result, n is not sensitive to α and the forward problem of ADI is highly sensitive to α. This makes estimation of these parameters cumbersome and non-unique when only pressure head data are used. The same applies to λ (Fig. 2b), which is difficult to predict because the objective function approaches its minimum value when α is close to its reference (0.0191 cm^{-1}).

An increase in α together with an increase in K_s leads to similar values for the objective function (Fig. 2c). Consequently, the forward problem of the ADI experiment has a high sensitivity to either α or K_s. There is a larger sensitivity to n–λ, n–K_s, and K_s–λ (Fig. 2d, 2e, and 2f, respectively). Observing the n–λ response surface, the objective function reaches a low value for n between 1.1 and 1.2, almost independent of λ between −3 and 3. Low values for the objective function also occur when λ is between −1.2 and −2 and n varies from 1.3 to 2.5. For the case of n–K_s (Fig. 2e), there is a large area of insensitivity, especially when both parameters are above their reference values (1.159 and 13.8 cm d^{-1}, respectively). There is no specific pattern for the sensitivity of the problem to the simultaneous variation of K_s and λ (Fig. 2f); however, low K_s with positive λ and high K_s with negative λ causes the objective function to increase.

Inverse Modeling Using Synthetic Data

The synthetic data obtained by forward modeling of a hypothetical ADI experiment on the three soil types from Table 1 are shown in Fig. 3a. As expected, a decrease in pressure head is faster and larger in the sandy soil. Temporal variation of the pressure head measured by tensiometers is the typical output of ADI experiments (Fig. 3a) and is used in inverse modeling to predict SHPs. Figure 3b shows a simulated measurement error imposed as a stochastic bias added to the numerically synthesized pressure head data (ADI output) for the silt soil.

The VG parameters estimated with and without added bias are shown in Table 3 together with their true values. The robustness

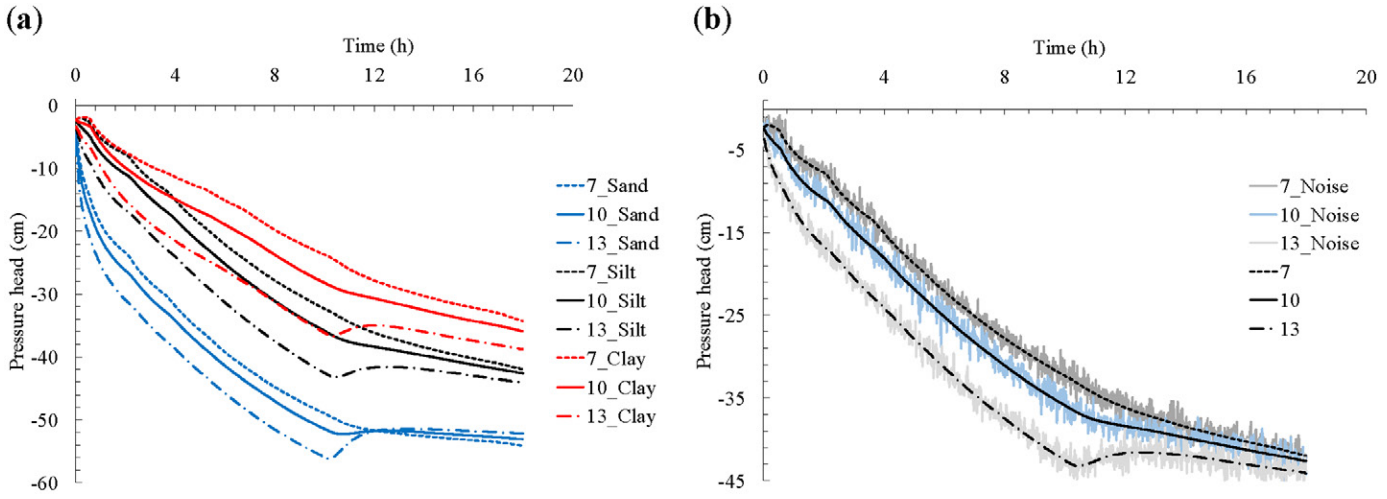

Fig. 3. (a) Simulated pressure head with time at three depths (7, 10, and 13 cm) in simulated automatic drip infiltrometer experiments for three soil types, and (b) example of the imposed stochastic bias added to the pressure heads for the silt soil.

Table 3. Soil hydraulic parameters estimated from synthesized data with and without added bias, together with true values for sand, silt, and clay reference soils.

Soil	Scenario	van Genuchten parameters†				RMSE$_h$‡
		α	n	K_s	λ	
		cm^{-1}		cm d^{-1}		cm
Sand	true value	0.0214	2.075	15.56	0.039	–
	estimated	0.0214	2.075	15.54	0.038	0.002
	estimated with bias	0.0213	2.10 (0.3)§	15.06	0.000 (0.006)	1.013
Silt	true value	0.0160	1.370	6.00	0.5	–
	estimated	0.0172	1.361	6.678	−0.001	0.018
	estimated with bias	0.0171	1.363	6.610	0.000	0.052
Clay	true value	0.0191	1.152	13.80	−1.384	–
	estimated	0.0191	1.152	13.80	−1.384	0.000
	estimated with bias	0.0182	1.154	12.83 (1.27)	−0.975 (0.333)	0.036

† θ_r, residual volumetric water content; θ_s, saturated volumetric water content; α, n, and λ, fitting parameters; K_s, saturated hydraulic conductivity.
‡ RMSE of pressure heads between scenario with true values and scenario with estimated values or estimated values with bias.
§ Standard deviation in parentheses if ≥0.5% of average value.

of the proposed experiment to estimate SHPs is confirmed, especially for sandy and clayey soils, with reference parameters equal or very close to the estimated parameters (Table 3). As mentioned by Peters and Durner (2008), prediction of the hydraulic conductivity function is the most crucial part.

Adding a small bias to the input data (as illustrated in Fig. 3b) introduced some uncertainties in the estimated parameters, as shown in Table 3, except for the silty soil parameters. Prediction of λ is cumbersome, occasionally with major differences between simulations with and without bias (sand soil) as well as large CVs (clay soil).

Pedotransfer Function

The developed GPR-PTF did not appear to be robust for the prediction of water contents at pF 1, but at pF 2, 3, and 4.2 well-trained GPR-PTFs were obtained for the training data set with, on average, RMSE and R^2 values of 0.015 and 0.99 for pF 2, 3, and 4.2, respectively, and the results of the testing stage are shown in Table 4. Feature selection of GPR based on kernel parameters allows elimination of predictors without a relevant effect on the response prediction (Kotlar et al., 2019a). Therefore, to predict θ_{pF2}, θ_{pF3} and $\theta_{pF4.2}$, two components of textural data (sand, sand and clay, or sand and silt content), organic matter content, and/or bulk density were important predictors. Their predictive role was of similar importance for θ_{pF2} and θ_{pF3} (Table 4); however, the silt fraction plays a more predominant role in the prediction of $\theta_{pF4.2}$.

Given the observed performance of the four PTFs, values of θ_{pF2}, θ_{pF3}, and $\theta_{pF4.2}$ for each experimental ADI soil column were predicted with the trained GPR-PTF and used as additional data for the drier part of the inverse simulation. The use of both pressure heads and water content data improves the well-posedness of the inverse problem (Kool and Parker, 1988).

Considering the bad performance of the respective PTF with R^2 and RMSE of 0.5 and 0.035 (Table 4), θ_{pF1} data were not used. This, however, was acceptable because many data from the ADI experiments were already available for very wet soil conditions. The average and CV of the measured soil parameters and estimated water contents for the 15 soil columns are given in Table 5.

Inverse Modeling of Actual Measurements

Addition of the water content data obtained from the developed PTF to the pressure head data from the ADI experiments resulted in proper estimation of VG parameters, as illustrated in Table 6. Although the columns were sampled from the same field, there is an extensive variation in VG parameters except for *n* (with a standard deviation of 0.08). Minimum and maximum values for α are 0.014 and 0.052 cm^{-1} and for λ are −1 to 24.4.

Table 4. Statistical indicators of performance of the Gaussian process regression pedotransfer functions for the prediction of volumetric water contents at pressure heads −0.1, −1, −10, and −158 m (θ_{pF1}, θ_{pF2}, θ_{pF3}, and $\theta_{pF4.2}$, respectively) for testing data and respective predictors (bulk density [BD], organic matter content [OM], and sand, silt, and clay contents).

	Targets			
Statistic	θ_{pF1}	θ_{pF2}	θ_{pF3}	$\theta_{pF4.2}$
R^2	0.534	0.952	0.894	0.946
RMSE	0.035	0.019	0.026	0.012
Predictors (weight in prediction)	BD (1.0)	BD (0.34) sand (0.34) OM (0.32)	BD (0.40) sand (0.35) clay (0.25)	silt (0.79) OM (0.20) sand (0.01)

There was no agreement between values of observed and simulated K_s. It should be remembered that K_s^{sim} values were obtained by inverse modeling from unsaturated columns, so they refer to extrapolation and are meant to be used for the prediction of unsaturated *K* values. The K_s^{obs} values (Table 6) were obtained from actual measurements in the laboratory. Similar findings were discussed by Pinheiro et al. (2018). Optimized parameters should be used only in the range where they were determined, and any extrapolation outside that range (as toward saturation) will be associated with a high level of uncertainty. Furthermore, there is spatial variability of K_s across small distances due to the variability and connectedness of macropores formed by root channels and earthworms or variability in bulk density (compaction) highlighted by Ghanbarian et al. (2017) and García-Gutiérrez et al. (2018). According to Table 6, the columns with the largest bulk density (>1.6 g cm^{-3}) were Columns 2, 3, and 15, corresponding to the lowest measured K_s. The highest values of K_s (9800, 5386, and 4068 cm d^{-1}) belong to Columns 13, 4, and 12, respectively, with an average bulk density of 1.45 g cm^{-3}.

When using only pressure head values in inverse modeling, no reliable SHPs were obtained. Values of RMSE for θ(*h*) are very high without using the GPR-PTF and reduce to more acceptable values when including the GPR-PTF water contents (Table 7). Because ADI data covered the wet range only, by excluding water content data no convergence was obtained for *K*(*h*) parameters, and the resulting retention parameters showed high errors in water content prediction (Table 7). In the predictions without GPR-PTF, unrealistic parameter prediction was frequently observed, and the inclusion of some water content values (θ_{pF2}, θ_{pF3}, $\theta_{pF4.2}$)

Table 5. Average and coefficient of variation (CV) of measured soil physical and hydraulic properties (sand, silt, and clay contents, organic matter content [OM], bulk density [BD], and saturated hydraulic conductivity [K_s]) and pedotransfer function-estimated water contents (θ) at pF2, 3, and 4.2 for 15 soil columns.

Parameter	Sand	Silt	Clay	OM	BD	K_s	θ_{pF2}	θ_{pF3}	$\theta_{pF4.2}$
	%				g cm^{-3}	log(cm d^{-1})			
Avg.	61.8	22.3	13.4	2.5	1.5	2.88	0.30	0.21	0.09
CV, %	3.5	3.9	9.1	7.5	4.9	122	3.9	7.0	8.4

Table 6. Estimated parameters obtained from inverse modeling of automatic drip infiltrometer experiments in 15 soil columns, including Gaussian process regression pedotransfer function water retention [θ(*h*)] values.

Column	Parameter†						
	θ_s	α	*n*	K_s^{sim}	K_s^{obs}	λ	BD
		cm^{-1}		——— cm d^{-1} ———			g m^{-3}
1	0.442	0.0360	1.342	186.8 (22.4)‡	532	5.9 (0.2)	1.48
2	0.381	0.0249	1.338	8.1 (0.2)	43	−0.02	1.64
3	0.381	0.0512	1.263	21.60	60	0.01	1.64
4	0.46	0.0515	1.269	29.6 (0.3)	5386.2	0.66	1.43
5	0.457	0.0141	1.552	5.9	2146	24.38 (1.47)	1.44
6	0.437	0.0391	1.275	7.1 (0.3)	845	0.001	1.49
7	0.479	0.0491	1.247	32.5 (0.2)	2680	−1.03	1.38
8	0.430	0.0360	1.372	9.6 (0.3)	494	0.014 (2.35)	1.51
9	0.415	0.0249	1.329	3.0 (0.2)	1447	0.02	1.55
10	0.453	0.0397	1.281	24.1 (1.8)	1735	−0.04	1.45
11	0.445	0.0395	1.298	75.6 (4.0)	834	1.14 (0.12)	1.47
12	0.456	0.0407	1.294	21.3 (1.7)	4068	3.10 (0.24)	1.44
13	0.445	0.0405	1.245	24.66 (1.0)	9829	−0.002 (0.24)	1.47
14	0.415	0.0379	1.251	20.9 (1.4)	373	0.001 (0.04)	1.55
15	0.392	0.0520	1.239	25.6	32	0.023	1.61

† θ_s, saturated volumetric water content; α, *n* and λ, fitting parameters; K_s, saturated hydraulic conductivity; BD, bulk density.
‡ Standard deviations in parentheses if ≥0.5% of true value.

Table 7. Statistical indicators of root mean square error (RMSE) and mean square percentage error (MSPE) for the performance of water retention [θ(*h*)] and hydraulic conductivity [*K*(*h*)] prediction by inverse modeling of automatic drip infiltrometer experiments in 15 soil columns including Gaussian process regression pedotransfer function (GPR-PTF) water contents and without GPR-PTF data.

Column	Including GPR-PTF			Without GPR-PTF†
	RMSE *K*(*h*)	MSPE *K*(*h*)	RMSE θ(*h*)	RMSE θ(*h*)
	cm d^{-1}			
1	9.6	39	0.034	0.125
2	0.2	30	0.037	0.030
3	0.8	126	0.036	0.046
4	2.3	176	0.025	0.117
5	4.5	48	0.046	0.189
6	0.1	260	0.052	0.164
7	0.9	1519	0.039	0.043
8	0.5	93	0.044	0.063
9	0.5	13	0.022	0.231
10	0.8	131	0.021	0.041
11	3.5	54	0.035	0.030
12	0.0	5	0.021	0.080
13	0.5	50	0.024	0.191
14	0.9	65	0.065	0.079
15	0.3	14	0.038	0.049

† For many cases, the van Genuchten parameters obtained from the scenarios without GPR-PTF did not result in reasonable values for *K*(*h*).

is required for proper estimation of θ(*h*) and *K*(*h*). Table 7 also evaluates the accuracy of simulated *K*(*h*) by Eq. [3] in terms of the RMSE and MSPE using the parameters in Table 6 compared with the observed values of *K*(*h*). Small values of *K*(*h*) or the dry-end tail of the *K*(*h*) function may be overestimated by the obtained SHPs. The RMSE is less able to detect this because absolute values of errors in the dry zone are small. The relative indicator MSPE expressed this more adequately.

Small values of the RMSE do not always indicate a proper prediction of *K*(*h*). For example, Columns 3, 7, and 10 correspond to similar RMSE values but resulted in very different values of MSPE (126, 1519, and 131, respectively). Similarly, the lowest RMSE value belongs to Column 6, with MSPE equal to 260.

Figure 4 shows the retention and hydraulic conductivity functions obtained in Soil Columns 7 and 12, the ones with the highest and lowest deviations, respectively, between measured values of *K* and those obtained by inverse modeling. In the retention graphs, the dashed line is obtained using the VG parameters from Table 6. In some cases, larger deviations occur between measured values of *K* and those obtained by inverse modeling in the drier part. This is the case, for example, for Soil Column 7, indicated in Fig. 4a by the red circle.

Finally, average and standard deviations of water retention data (θ_s, θ_{pF1}, θ_{pF2}, θ_{pF3}, $\theta_{pF4.2}$) measured by steady-state methods on small rings with those obtained from inverse modeling of ADI+PTF performed on large columns are compared in Fig. 5. The difference between measured and simulated water

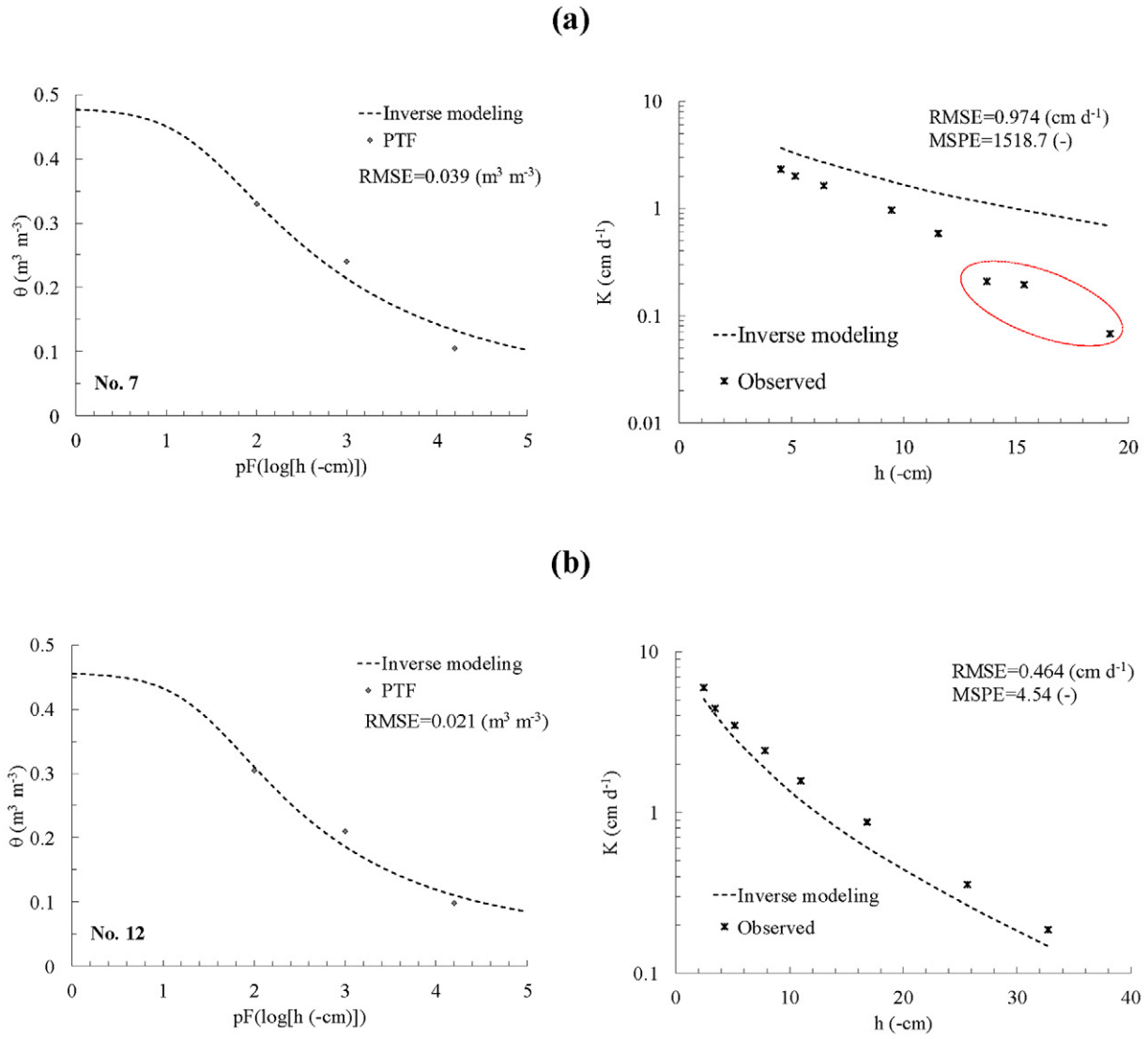

Fig. 4. Water retention [θ(*h*)] and hydraulic conductivity functions obtained in (a) Soil Column 7, the column with the highest deviation between hydraulic conductivity *K* measured and obtained by inverse modeling, and (b) Soil Column 12, with the lowest respective deviation. The red circle in (a) shows the high deviation for some of the observed values; PTF, pedotransfer function; MSPE, mean square percentage error.

contents for the drier soil (θ_{pF3} and $\theta_{pF4.2}$) is larger than for the wetter values. The water contents estimated by steady-state methods were higher than those inversely obtained from the ADI experiments. Differences increased to about 0.05 $m^3\ m^{-3}$ in the drier region.

Conclusions

The evaluation of automated drip infiltrometer (ADI) scenarios performed here in numerical and real experiments to obtain soil hydraulic parameters from inverse modeling led to the following conclusions:

- Evaluated for three reference soils, the inverse modeling of ADI experiments showed insensitivity to residual and saturated water content. These parameters can better be measured or estimated than predicted from these experiments.

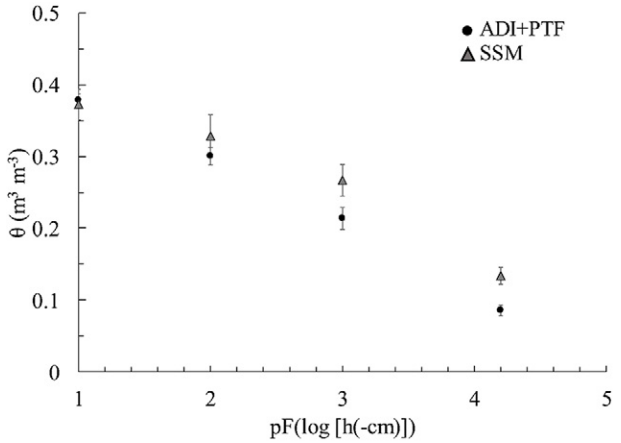

Fig. 5. Average of water content θ at pF1, pF2, pF3, and pF4 obtained from steady-state methods (SSM) vs. corresponding values obtained from inverse modeling of automatic drip infiltrometer (ADI) + pedotransfer function (PTF).

- A numerical simulation of ADI scenarios showed robust prediction of soil hydraulic parameters by inverse modeling. Introduction of a random error to input data did not affect the parameter estimation notably.
- Including water contents predicted for the drier soil by a GPR-PTF for the inverse modeling ADI data from 15 large undisturbed columns collected from the same field located in Denmark, van Genuchten parameters α, K_s, n, and λ were uniquely identified and the unsaturated hydraulic conductivities calculated from these data were in good agreement with measured $K(h)$. Not including the PTF water contents resulted in non-uniquely estimated van Genuchten parameters.

Data Availability

Data from this study are available through the Dryad Data Depository (Kotlar et al., 2019d).

Acknowledgments

A.M. Kotlar is grateful to the FAPESP Foundation, Brazil, for providing financial support (scholarship) for his study (process no. 2016/18636-7). The support from the Danish Environment Agency financed project Mapping of Risk Areas for Phosphorus Loss and Phosphorus Sensitive Water Areas (Fosforkortlaegning) and from the Danish Pesticide Leaching Assessment Programme (pesticidvarsling.dk) is gratefully acknowledged. We also acknowledge two anonymous reviewers who contributed greatly to the manuscript during the reviewing process.

References

Arora, B., B.P. Mohanty, and J.T. McGuire. 2011. Inverse estimation of parameters for multidomain flow models in soil columns with different macropore densities. Water Resour. Res. 47:W04512. doi:10.1029/2010WR009451

Bouma, J., F.G. Baker, and P.L.M. Veneman. 1974. Measurement of water movement in soil pedons above the water table. Inf. Circ. 27. Geol. and Nat. Hist. Surv., Univ. of Wisconsin, Madison.

Durner, W., E. Priesack, H.-J. Vogel, and T. Zurmühl. 1999. Determination of parameters for flexible hydraulic functions by inverse modeling. In: M.Th. van Genuchten et al., editors, Proceedings of the International Workshop on Characterization and Measurement of the Hydraulic Properties of Unsaturated Porous Media, Riverside, CA. 22–24 Oct. 1997. Univ. of California, Riverside. p. 817–829.

García-Gutiérrez, C., Y. Pachepsky, and M.Á. Martin. 2018. Saturated hydraulic conductivity and textural heterogeneity of soils. Hydrol. Earth Syst. Sci. 22:3923–3932. doi:10.5194/hess-2017-706

Gardner, W.R., and F.J. Miklich. 1962. Unsaturated conductivity and diffusivity measurements by a constant flux method. Soil Sci. 93:271–274. doi:10.1097/00010694-196204000-00008

Ghanbarian, B., V. Taslimitehrani, and Y.A. Pachepsky. 2017. Accuracy of sample dimension-dependent pedotransfer functions in estimation of soil saturated hydraulic conductivity. Catena 149:374–380. doi:10.1016/j.catena.2016.10.015

Graham, S.L., M.S. Srinivasan, N. Faulkner, and S. Carrick. 2018. Soil hydraulic modeling outcomes with four parameterization methods: Comparing soil description and inverse estimation approaches. Vadose Zone J. 17:170002. doi:10.2136/vzj2017.01.0002

Groh, J., C. Stumpp, A. Lücke, T. Pütz, J. Vanderborght, and H. Vereecken. 2018. Inverse estimation of soil hydraulic and transport parameters of layered soils from water stable isotope and lysimeter data. Vadose Zone J. 17:170168. doi:10.2136/vzj2017.09.0168

Hopmans, J.W., D.R. Nielsen, and K.L. Bristow. 2002. How useful are small-scale soil hydraulic property measurements for large-scale vadose zone modeling? Geophys. Monogr. 129:247–258. doi:10.1029/129GM20

Hudson, D.B., P.J. Wierenga, and R.G. Hills. 1996. Unsaturated hydraulic properties from upward flow into soil cores. Soil Sci. Soc. Am. J. 60:388–396. doi:10.2136/sssaj1996.03615995006000020009x

Iversen, B.V., M. Koppelgaard, and O.H. Jacobsen. 2004. An automated system for measuring air permeability and hydraulic conductivity in the laboratory on large soil cores. DIAS Report, Plant Prod. 111. Danish Inst. of Agric. Sci., Tjele.

Kelleners, T.J., R.W.O. Soppe, J.E. Ayars, J. Šimůnek, and T.H. Skaggs. 2005. Inverse analysis of upward water flow in a groundwater table lysimeter. Vadose Zone J. 4:558–572. doi:10.2136/vzj2004.0118

Kool, J.B., and J.C. Parker. 1988. Analysis of the inverse problem for transient unsaturated flow. Water Resour. Res. 24:817–830. doi:10.1029/WR024i006p00817

Kool, J.B., J.C. Parker, and M.Th. van Genuchten. 1985. Determining soil hydraulic properties from one-step outflow experiments by parameter estimation: I. Theory and numerical studies. Soil Sci. Soc. Am. J. 49:1348–1354. doi:10.2136/sssaj1985.03615995004900060004x

Kotlar, A.M., B.V. Iversen, and Q. de Jong van Lier. 2019a. Evaluation of parametric and nonparametric machine-learning techniques for prediction of saturated and near-saturated hydraulic conductivity. Vadose Zone J. 18:180141. doi:10.2136/vzj2018.07.0141

Kotlar, A.M., B.V. Iversen, and Q. de Jong van Lier. 2019b. Data from: Evaluation of parametric and nonparametric machine-learning techniques for prediction of saturated and near-saturated hydraulic conductivity. Dryad Digital Repository. doi:10.5061/dryad.ph0b6k8

Kotlar, A.M., B.V. Iversen, and Q. de Jong van Lier. 2019c. Machine learning-based prediction of drainage in layered soils using a soil drainability index. Soil Syst. 3:30. doi:10.3390/soilsystems3020030

Kotlar, A.M., I. Varvaris, Q. de Jong van Lier, L.W. de Jonge, P. Møldrup, and B.V. Iversen. 2019d. Data from: Soil hydraulic properties determined by inverse modeling of drip infiltrometer experiments extended with pedotransfer functions. Dryad Digital Depository. doi:10.5061/dryad.7q22r2m

Lambot, S., F. Hupet, M. Javaux, and M. Vanclooster. 2004. Laboratory evaluation of a hydrodynamic inverse modeling method based on water content data. Water Resour. Res. 40:W03506. doi:10.1029/2003WR002641

Li, Y.-B., Y. Liu, W.-B. Nie, and X.-Y. Ma. 2018. Inverse modeling of soil hydraulic parameters based on a hybrid of vector-evaluated genetic algorithm and particle swarm optimization. Water 10:84. doi:10.3390/w10010084

Lindhardt, B., C. Abildtrup, H. Vosgerau, P. Olsen, S. Torp, B.V. Iversen, et al. 2001. The Danish pesticide leaching assessment programme: Site characterization and monitoring description. Geol. Surv. of Denmark and Greenland, Copenhagen.

Mallants, D., B.P. Mohanty, A. Vervoort, and J. Feyen. 1997. Spatial analysis of saturated hydraulic conductivity in a soil with macropores. Soil Technol. 10:115–131. doi:10.1016/S0933-3630(96)00093-1

McKenzie, N.J., H.P. Cresswell, H. Rath, and D. Jacquier. 2001. Measurement of unsaturated hydraulic conductivity using tension and drip infiltrometers. Aust. J. Soil Res. 39:823–836. doi:10.1071/SR99136

Moret-Fernández, D., B. Latorre, C. Peña-Sancho, and T.A. Ghezzehei. 2016. A modified multiple tension upward infiltration method to estimate the soil hydraulic properties. Hydrol. Processes 30:2991–3003. doi:10.1002/hyp.10827

Pachepsky, Y., and R.L. Hill. 2017. Scale and scaling in soils. Geoderma 287:4–30. doi:10.1016/j.geoderma.2016.08.017

Peters, A., and W. Durner. 2008. Simplified evaporation method for determining soil hydraulic properties. J. Hydrol. 356:147–162. doi:10.1016/j.jhydrol.2008.04.016

Pinheiro, E.A.R., Q. de Jong van Lier, and K. Metselaar. 2018. A matric flux potential approach to assess plant water availability in two climate zones in Brazil. Vadose Zone J. 17:160083. doi:10.2136/vzj2016.09.0083

Rashid, N.S.A., M. Askari, T. Tanaka, J. Šimůnek, and M.Th. van Genuchten. 2015. Inverse estimation of soil hydraulic properties under oil palm trees. Geoderma 241–242:306–312. doi:10.1016/j.geoderma.2014.12.003

Rasmussen, C.E., and C.K.I. Williams. 2006. Gaussian processes for machine learning. MIT Press, Cambridge, MA.

Ritter, A., F. Hupet, R. Muñoz-Carpena, S. Lambot, and M. Vanclooster. 2003. Using inverse methods for estimating soil hydraulic properties

from field data as an alternative to direct methods. Agric. Water Manage. 59:77–96. doi:10.1016/S0378-3774(02)00160-9

Romano, N., and A. Santini. 1999. Determining soil hydraulic functions from evaporation experiments by a parameter estimation approach: Experimental verifications and numerical studies. Water Resour. Res. 35:3343–3359. doi:10.1029/1999WR900155

Scharnagl, B., J.A. Vrugt, H. Vereecken, and M. Herbst. 2011. Inverse modelling of in situ soil water dynamics: Investigating the effect of different prior distributions of the soil hydraulic parameters. Hydrol. Earth Syst. Sci. 15:3043–3059. doi:10.5194/hess-15-3043-2011

Schelle, H., S.C. Iden, and W. Durner. 2011. Combined transient method for determining soil hydraulic properties in a wide pressure head range. Soil Sci. Soc. Am. J. 75:1681–1693. doi:10.2136/sssaj2010.0374

Šimůnek, J., M. Šejna, H. Saito, M. Sakai, and M.Th. van Genuchten. 2008. The HYDRUS-1D software package for simulating the movement of water, heat, and multiple solutes in variably saturated media, version 4.0. HYDRUS Softw. Ser. 3. Dep. of Environ. Sci., Univ. of California, Riverside.

Šimůnek, J., M.Th. van Genuchten, and M. Šejna. 2005. The HYDRUS-1D software package for simulating the one-dimensional movement of water, heat, and multiple solutes in variably-saturated media. Res. Rep. 3. Univ. of California, Riverside.

Šimůnek, J., M.Th. van Genuchten, and O. Wendroth. 1998. Parameter estimation analysis of the evaporation method for determining soil hydraulic properties. Soil Sci. Soc. Am. J. 62:894–905. doi:10.2136/sssaj1998.03615995006200040007x

van Dam, J.C., J.N.M. Stricker, and P. Droogers. 1994. Inverse method to determine soil hydraulic functions from multistep outflow experiments. Soil Sci. Soc. Am. J. 58:647–652. doi:10.2136/sssaj1994.03615995005800030002x

van Dam, J.C., J.N.M. Stricker, and P. Droogers. 1992. Inverse method for determining soil hydraulic functions from one-step outflow experiments. Soil Sci. Soc. Am. J. 56:1042–1050. doi:10.2136/sssaj1992.03615995005600040007x

van Genuchten, M.Th. 1980. A closed-form equation for predicting the hydraulic conductivity of unsaturated soils. Soil Sci. Soc. Am. J. 44:892–898. doi:10.2136/sssaj1980.03615995004400050002x

Vrugt, J.A., W. Bouten, and A.H. Weerts. 2001. Information content of data for identifying soil hydraulic parameters from outflow experiments. Soil Sci. Soc. Am. J. 65:19–27. doi:10.2136/sssaj2001.65119x

Weller, U., O. Ippisch, M. Köhne, and H.-J. Vogel. 2011. Direct measurement of unsaturated conductivity including hydraulic nonequilibrium and hysteresis. Vadose Zone J. 10:654–661. doi:10.2136/vzj2010.0074

Weninger, T., G. Bodner, J. Kreiselmeier, P. Chandrasekhar, S. Julich, K.-H. Feger, et al. 2018. Combination of measurement methods for a wide-range description of hydraulic soil properties. Water 10:1021. doi:10.3390/w10081021

Wind, G.P. 1969. Capillary conductivity data estimated by a simple method. In: P.E. Rijtema and H. Wassink, editors, Water in the Unsaturated Zone: Proceedings of the Wageningen Symposium, Wageningen, the Netherlands. June 1966. Vol. 1. UNESCO, Paris. p. 181–190.

Young, M.H., A. Karagunduz, J. Šimůnek, and K.D. Pennell. 2002. A modified upward infiltration method for characterizing soil hydraulic properties. Soil Sci. Soc. Am. J. 66:57–64. doi:10.2136/sssaj2002.5700

Zhang, Z.F., A.L. Ward, and G.W. Gee. 2003. Estimating soil hydraulic parameters of a field drainage experiment using inverse techniques. Vadose Zone J. 2:201–211. doi:10.2136/vzj2003.2010